Mg^{2+} and memantine block of rat recombinant NMDA receptors containing chimeric NR2A/2D subunits expressed in *Xenopus laevis* oocytes

David C. Wrighton, Edward J. Baker, Philip E. Chen and David J. A. Wyllie

Centre for Neuroscience Research, Hugh Robson Building, University of Edinburgh, George Square, Edinburgh EH8 9XD, UK

N-methyl-D-aspartate receptors (NMDARs) display differences in their sensitivity to the channel blockers Mg^{2+} and memantine that are dependent on the identity of the NR2 subunit present in the receptor–channel complex. This study used two-electrode voltage-clamp recordings from *Xenopus laevis* oocytes expressing recombinant NMDARs to investigate the actions of Mg^{2+} and memantine at the two NMDARs displaying the largest differences in sensitivity to these blockers, namely NR1/NR2A and NR1/NR2D NMDARs. In addition, NR2A/2D chimeric subunits have been employed to examine the effects of pore-forming elements and ligand-binding domains (LBD) on the potency of the block produced by each of these inhibitors. Our results show that, as previously documented, NR2D-containing NMDARs are less sensitive to voltage-dependent Mg^{2+} block than their NR2A-containing counterparts. The reduced sensitivity is determined by the M1M2M3 membrane-associated regions, as replacing these regions in NR2A subunits with those found in NR2D subunits results in a ∼10-fold reduction in Mg^{2+} potency. Intriguingly, replacing the NR2A LBD with that from NR2D subunits results in a ∼2-fold increase in Mg^{2+} potency. Moreover, when responses mediated by NR1/NR2A NMDARs are evoked by the partial agonist homoquinolinate, rather than glutamate, Mg^{2+} also displays an increased potency. Memantine block of glutamate-evoked currents is most potent at NR1/NR2D NMDARs, but no differences are observed in its ability to inhibit NR2A-containing or NR2A/2D chimeric NMDARs. We suggest that the potency of block of NMDARs by Mg^{2+} is influenced not only by pore-forming regions but also the LBD and the resulting conformational changes that occur following agonist binding.

(Received 20 August 2007; accepted after revision 23 October 2007; first published online 25 October 2007)
Corresponding author D. J. A. Wyllie: Centre for Neuroscience Research, Hugh Robson Building, University of Edinburgh, George Square, Edinburgh EH8 9XD, UK. Email: dwyllie1@staffmail.ed.ac.uk

N-methyl-D-aspartate receptors (NMDARs) possess two key features that allow them to play pivotal roles in physiological and pathophysiological functions in the mammalian central nervous system (CNS). The first of these is their high permeability to Ca^{2+} ions. Flow of Ca^{2+} ions through NMDARs is a trigger for the activation of biochemical cascades that mediate processes such as synaptogenesis, excitotoxicity, synaptic plasticity and learning and memory (for a review see Dingledine *et al.* 1999). The second is their sensitivity to Mg^{2+} ions which block the ion channel pore of NMDARs in a voltage-dependent manner (Mayer *et al.* 1984; Nowak *et al.* 1984). The voltage dependence of this block allows NMDARs to act as 'coincidence detectors' (Bliss & Collingridge, 1993) whereby they mediate ion flow when the membrane potential of the cell is sufficiently depolarized to relieve the channel blocking effects of Mg^{2+} ions.

The majority of NMDARs in the CNS are composed of two NR1 and two NR2 subunits. The NR1 subunit can exist in eight splice isoforms, contains the binding site for the coagonist, glycine, whose presence in the NMDAR complex is essential for a functional receptor–channel to be formed. NR2 subunits are derived from four separate gene products (NR2A–D) and contain the binding site for glutamate (for reviews see Dingledine *et al.* 1999; Cull-Candy *et al.* 2001; Erreger *et al.* 2004; Chen & Wyllie, 2006). The expression of NR2 subunits is regulated both developmentally and temporally (Monyer *et al.* 1994) and the inclusion of particular NR2 subunits in NMDARs imparts the majority of the pharmacological and biophysical properties associated

D. C. Wrighton and E. J. Baker contributed equally to this work. This paper has online supplemental material.

 DOI: 10.1113/jphysiol.2007.143164

with each of the various NMDAR subtypes (Monyer *et al.* 1992, 1994; Ishii *et al.* 1993; Vicini *et al.* 1998; Wyllie *et al.* 1998).

Of particular interest to this present study are the differences in potency of Mg^{2+} block at each of the recombinant NMDAR subtypes (Monyer *et al.* 1992; Kuner & Schoepfer, 1996). Indeed differences in the ability of Mg^{2+} to block NMDARs found in different brain regions and/or at different developmental stages have also been observed (Kleckner & Dingledine, 1991; Kato & Yoshimura, 1993; Nabekura *et al.* 1994). Thus, NR2A- and NR2B-containing NMDARs are more sensitive to Mg^{2+} block than NMDARs that contain NR2C or NR2D subunits. Nevertheless all four NMDAR subunits possess an asparagine (N) residue at the so-called 'QRN site' (Burnashev *et al.* 1992; Mori *et al.* 1992; Sakurada *et al.* 1993) and at the N_{+1} site (Wollmuth *et al.* 1998) indicating that additional structural elements are required to determine the overall sensitivity of an NMDAR subtype to block by Mg^{2+}. Using a chimeric approach to produce an NR1/NR2C NMDAR with the Mg^{2+} sensitivity of an NR1/NR2B NMDAR, Kuner & Schoepfer (1996) identified three additional regions that when taken from NR2B subunits and substituted into NR2C subunits produced an NR1/NR2B/2C chimeric NMDAR with a Mg^{2+} sensitivity similar to that seen with NR1/NR2B NMDARs. These segments were the M1 domain, M2–M3 linker and M4 domain. They concluded that these three elements, together with the M2 region itself were the determinants of the nature of the Mg^{2+} block seen at various NMDAR subtypes.

NMDARs can be considered to contain a series of functional domains (Dingledine *et al.* 1999; Mayer & Armstrong, 2004; Chen & Wyllie, 2006; Mayer, 2006; Fig. 1*A*. These can be defined as the following: the extracellularly located amino terminal domain (ATD), which contains sites of action of several allosteric modulators of NMDAR function; the ligand binding domain (LBD), which is created by two regions termed S1 and S2 that come together to form a bi-lobar structure; the membrane-associated regions (M1–M4); and the intracellularly located carboxy terminal domain (CTD), which interacts with a large number of proteins to initiate biochemical cascades following NMDAR activation. In the present study we have examined the influence of both the LBD and membrane-associated domain on the channel block produced by Mg^{2+} when NMDARs are activated by glutamate itself and by homoquinolinate, a partial agonist

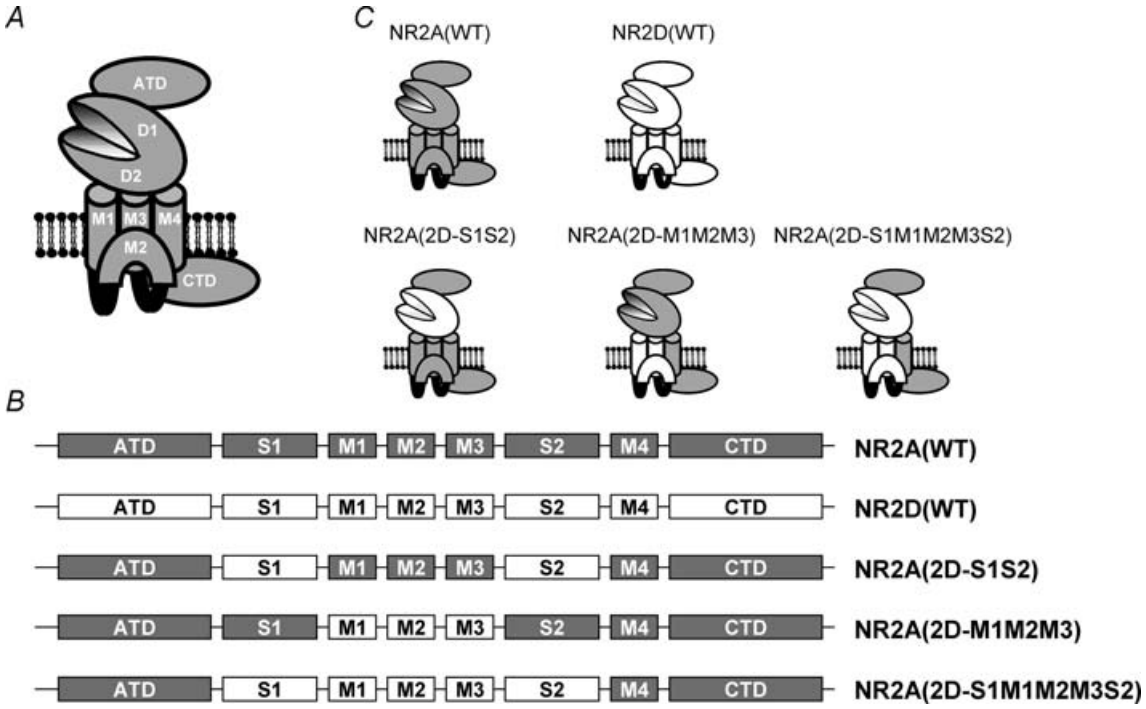

Figure 1. Cartoon illustration of an NMDAR subunit and the various chimeric constructs examined
A, cartoon sketch of an ionotropic glutamate receptor subunit showing the proposed membrane topology of three membrane spanning domains (M1, M3 and M4) and a re-entrant loop (M2), and the location of the amino terminal domain (ATD) and carboxy terminal domain (CTD). The ligand binding domains (denoted D1 and D2) are formed by the S1 and S2 regions of the protein, which come together to form a hinged clamshell-like structure. *B*, linear representation of the various NMDAR constructs investigated and the nomenclature used in this study. Regions originating from the NR2A subunit are shown in grey, while those originating from the NR2D subunit are shown in white. *C*, cartoon representation of these constructs showing how the various functional domains from the NR2D subunit are incorporated into the three chimeric subunits.

at NR2A-containing NMDARs (Erreger *et al.* 2005). The effects of memantine, another NMDAR channel blocker, used therapeutically in the treatment of dementia, have also been investigated (Parsons *et al.* 1993, 1999*b*; Chen & Lipton, 2005; Lipton, 2006). In addition we have created chimeric subunits where we have swapped LBDs and membrane-associated domains found in NR2A subunits with the equivalent regions present in NR2D subunits to investigate the effects these structural elements have on the block produced by these two channel blockers.

In agreement with previous studies (Monyer *et al.* 1992; Kuner & Schoepfer, 1996) our results indicate that Mg^{2+} is less potent at blocking NR1/NR2D NMDAR-mediated responses than those mediated by NR1/NR2A NMDARs and that this reduced sensitivity to Mg^{2+} is determined by pore-forming elements of the receptor–channel. However two additional findings concerning Mg^{2+} block are reported. First, Mg^{2+} gives a more potent block of NMDAR-mediated currents when these responses are evoked by the partial agonist homoquinolinate, and second, inclusion of the NR2D LBD in NR2A subunits also leads to an increase in Mg^{2+} potency. Channel block by memantine is most potent at NR1/NR2D NMDARs, but substituting either the LBD or the membrane-associated regions of NR2D subunits into NR2A subunits does not give rise to a receptor–channel displaying 'NR2D-like' memantine block. The results presented in this study complement those in our accompanying paper (Chen *et al.* 2007) and together provide evidence that the LBD of NR2 subunits influences two characteristic properties of NMDARs, namely coagonist binding/potency (Chen *et al.* 2007) and voltage-dependent Mg^{2+} block (this study).

Methods

Plasmid constructs, cRNA synthesis and receptor expression in oocytes

The amino acid numbering system we use here is consistent with our previous publications investigating structure–function relationships in recombinant NMDARs and refers to the position of residues in the mature protein (i.e. the signal peptide is excluded). The wild-type pSP64T-derived expression plasmids for rodent NR1 and NR2 NMDA receptor subunits were as previously described (Chen *et al.* 2005; Wyllie *et al.* 2006). In this study we coexpressed NR2A, NR2D and chimeric NR2A/D NMDAR subunits with the NR1–1a (exon 5 lacking, exon 21, 22 containing) subunit (Hollmann *et al.* 1993), which we will refer to as 'NR1'. Chimeras of NR2A and NR2D subunits were generated using a PCR-based strategy (Chen *et al.* 2007; Erreger *et al.* 2007). The NR2A(2D-S1S2) chimera was generated by replacing Val370–Val518 in the NR2A subunit with Leu389–Val539 from the NR2D subunit and by replacing Glu638–Ile795 in the NR2A subunit with Glu659–Ile816 from the NR2D subunit. In addition to this 'binding site' chimera, we also generated a chimera in which the NR2A M1, M2 and M3 membrane associated regions (residues Ser519–Glu638) were replaced by those found in the NR2D subunit (Arg541–Glu658) We refer to this chimera as NR2A(2D-M1M2M3). The NR2A(2D-S1M1M2M3S2) chimera replaced both the NR2A ligand-binding domain and first three membrane-associated regions with those found in the NR2D subunit. Linear representations and cartoon depictions of these constructs are shown in Fig. 1*B* and *C*. All inserted PCR-generated DNA segments and subcloning sites were confirmed by DNA sequencing. cRNA was synthesized as runoff transcripts from restriction endonuclease (Mlu I or Not I) linearized plasmid DNA using the Promega RiboMax RNA synthesis kit (Promega, Madison, WI, USA) or mMessage Machine (Ambion, Warrington, UK). Reactions were supplemented with 0.75 mM capping nucleotide $m^7G(5')ppp(5')G$ (Promega) in the presence of 1.6 mM GTP. cRNA amounts and integrity were estimated by intensity of fluorescence in ethidium bromide-stained agarose gels. NR1 and NR2 cRNAs were mixed at a nominal ratio ranging between 1 : 1 and 1 : 9, with the NR1 content being 5 ng.

Stage V–VI oocytes were obtained from *Xenopus laevis* that had been anaesthetized by immersion in a solution of 3-amino-benzoic acid ethylester (0.5%) and then killed by injection of an overdose solution of pentobarbital (0.4 ml of a 20% solution) followed by decapitation and exsanguation after the confirmation of loss of cardiac output. All procedures were carried out in accordance with current UK Home Office regulations. Prior to injection with cRNA mixtures of interest, the follicular membranes of the oocytes were removed. After injection oocytes were placed in separate wells of 24-well plates containing a modified Barth's solution with composition (mM): NaCl 88, KCl 1, $NaHCO_3$ 2.4, $MgCl_2$ 0.82, $CaCl_2$ 0.77, Tris-Cl 15, adjusted to pH 7.35 with NaOH. This solution was supplemented with 50 IU ml^{-1} penicillin and 50 $\mu g\,ml^{-1}$ streptomycin (Invitrogen, Paisley, UK). Oocytes were placed in an incubator (19°C) for 24–48 h to allow for receptor expression and then stored at 4°C until required for electrophysiological measurements.

Electrophysiological recordings and solutions

Two electrode voltage clamp (TEVC) recordings were made using a GeneClamp 500 amplifier (Molecular Devices, Union City, CA, USA), from oocytes that were placed in a solution that contained (mM): NaCl 115, KCl 2.5, Hepes 10, $BaCl_2$ 1.8, EDTA 0.01; pH 7.3 with NaOH (20°C) (Sigma-Aldrich, Poole, UK). EDTA (10 μM) was added to chelate contaminant extracellular divalent ions, including trace amounts of Zn^{2+}. Current and voltage

electrodes were made from thin-walled borosilicate glass (GC150TF-7.5, Harvard Apparatus, Edenbridge, UK) using a PP-830 electrode puller (Narashige Instruments, Japan) and when filled with 3 M KCl possessed resistances of between 0.5 and 1.5 MΩ. Oocytes were voltage-clamped at potentials between −80 and +10 mV in increments of 10 mV for the generation of current–voltage plots and at −40, −60 and −80 mV when investigating the inhibition of NMDAR-mediated responses by Mg^{2+} ions or memantine. Glycine (50 μM) was added to all glutamate- or homoquinolinate-containing solutions to ensure that the glycine binding site located on the NR1 NMDAR subunit was saturated. Thus, when we refer to glutamate- or homoquinolinate-evoked responses below, we should be taken to mean that these solutions contained, in addition to the NR2 agonist, glycine (50 μM). For most experiments the glutamate concentration was set to be equal to the EC_{50} for this agonist at NR1/NR2A NMDARs (3 μM), while homoquinolinate was used at a concentration of 10 μM. These concentrations, while producing robust responses in oocytes expressing recombinant NMDARs, give more stable responses than do higher concentrations which normally lead to 'sag' in the NMDAR-mediated response over the prolonged recording periods required to generate a series of inhibition curves at three different holding potentials. Application of solutions was controlled manually and agonist-evoked currents were filtered at 10 Hz and digitized at 100 Hz via CED 1401-plus (CED, Cambridge, UK) or Digidata 1200 (Molecular Devices, Union City, CA, USA) A/D interfaces using WinEDR software (Strathclyde Electrophysiology Software, Strathclyde University, UK). Solutions were applied for 20–60 s or until a plateau to the response had been achieved. All chemicals were purchased from Sigma-Aldrich (Poole, UK) with the exception of homoquinolinic acid and memantine (Tocris Bioscience, Bristol, UK).

Analysis of concentration and voltage dependence of Mg^{2+} and memantine block of NMDAR-mediated currents

Individual concentration–response (inhibition) curves for Mg^{2+} and memantine block of NMDAR-mediated responses obtained at holding potentials of −40, −60 and −80 mV were fitted with the following equation:

$$I = I_{max}/\left(1 + ([B]/IC_{50})^{n_H}\right), \quad (1)$$

where n_H is the Hill coefficient, I_{max} is the predicted maximum current (in the absence of blocker), [B] is the concentration of blocker, and IC_{50} is the concentration of the blocker that produces a half-maximum inhibition of the agonist-evoked response. Each data point was then normalized to the predicted fitted maximum of the concentration–response curve. These normalized values were then pooled and averaged for each construct and fitted again with the above equation, with the maximum constrained to asymptote to 1. The minimum was not constrained, unless a negative value was predicted from the fit, when, under such circumstances, the data were re-fitted with the minimum constrained to asymptote to 0 (Frizelle *et al.* 2006).

The voltage dependence of Mg^{2+} and memantine block of NMDAR-mediated responses was determined by calculating values of δ, the fraction of the electric field that the blocker experiences, from the estimates of IC_{50} values obtained at −40, −60 and −80 mV according to the Woodhull equation (Woodhull, 1973):

$$K_{d,V} = K_{d,0\,mV} e^{(z\delta VF/RT)}, \quad (2)$$

where z is valency of the blocker (+2 for Mg^{2+} and +1 for memantine), V is membrane potential, R is the gas constant, T is absolute temperature and F is Faraday's constant. The relationship between the equilibrium constant, K_d, for a blocker and its IC_{50} value is model dependent and it is not necessarily the case that these two parameters will be equal (Wyllie & Chen, 2007). While it has been reported that for Mg^{2+} block these two values are similar (Qian *et al.* 2002), which suggests that Mg^{2+} ions do not alter channel gating, we have used eqn (2) to estimate only δ values for each NMDAR construct. Such values can be estimated if we assume that the relationship between IC_{50} and K_d values is independent of voltage, and receptor activation itself is not voltage dependent. We did not, however, obtain estimates of the $K_{d,0mV}$ for Mg^{2+} or memantine by substituting for $K_{d,V}$ values the corresponding IC_{50} values obtained at the respective voltages.

Statistical analysis

Two-way ANOVA and Student's t test (GraphPad Prism v4.0, GraphPad Software Inc., San Diego, CA, USA) were used to determine whether significant differences ($P < 0.05$) existed between IC_{50} and δ values for Mg^{2+} and memantine at each of the NMDAR constructs examined. The mean values and errors we report are those estimated from the fitting of the mean pooled datasets (Origin v6.0; OriginLab Corp., Northampton, MA, USA).

Results

Voltage-dependent block of glutamate- and homoquinolinate-evoked currents by Mg^{2+} ions

Throughout this study we have investigated voltage-dependent Mg^{2+} block of NMDAR-mediated currents at three holding potentials, namely −80, −60

and −40 mV. Figure 2*A* shows a typical series of TEVC traces recorded from an oocyte expressing NR1/NR2A NMDARs where application of glutamate (3 μM) evokes inward currents that are blocked, reversibly, when the bathing solution contains Mg^{2+} (100 μM). As exemplified in Fig. 2*B*, where the initial steady-state currents evoked at the holding potentials of −60 and −40 mV have been scaled to that obtained at −80 mV, the extent of the block by Mg^{2+} decreases as the membrane potential is depolarized.

To determine the concentration of Mg^{2+} required to block wild-type and chimeric NMDAR-mediated

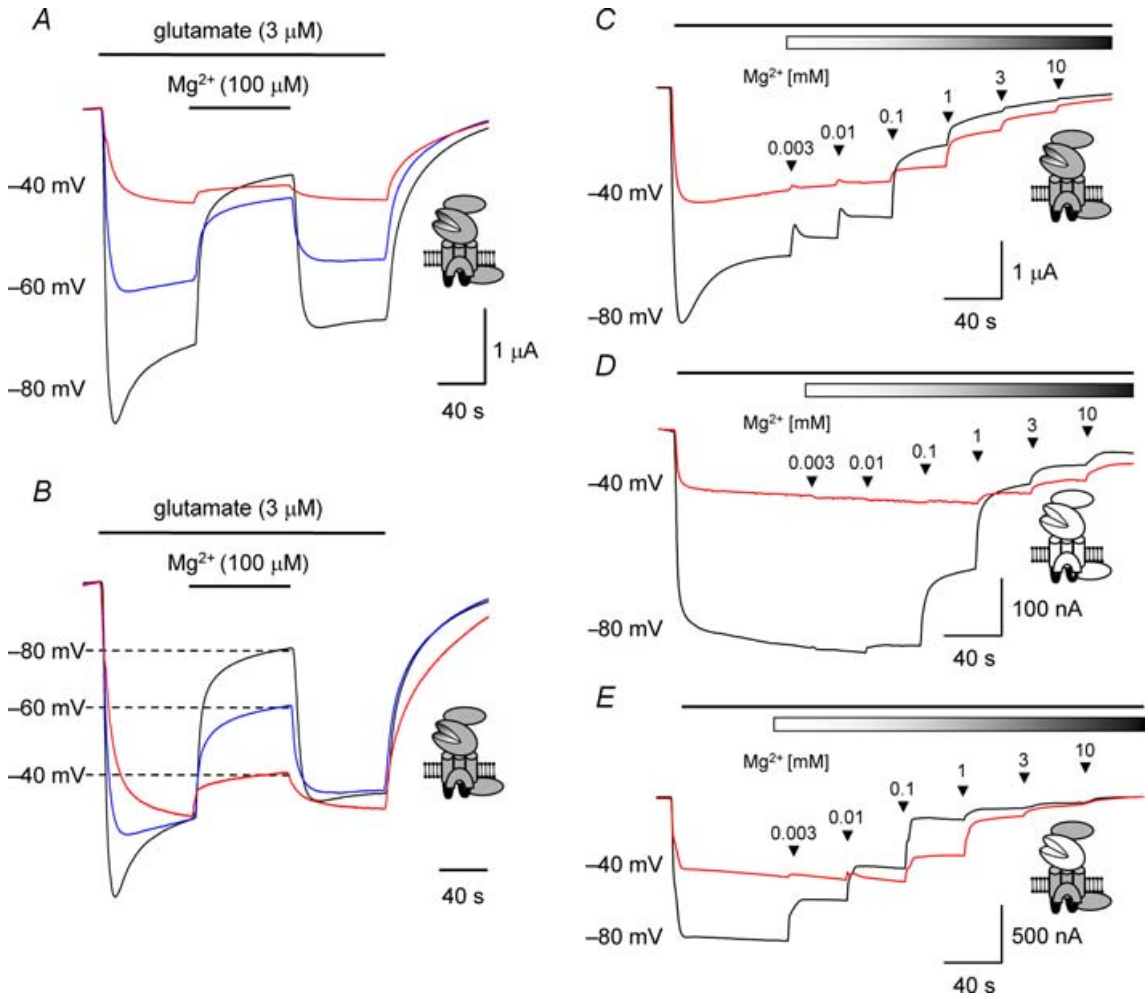

Figure 2. TEVC current recordings illustrating voltage and concentration dependence of Mg^{2+} block in wild-type and chimeric NMDARs

A, example TEVC traces recorded from an oocyte expressing NR1/NR2A NMDARs The glutamate-evoked currents recorded at each of the membrane potentials indicated are reversibly inhibited by coapplication of Mg^{2+} (100 μM) at the point indicated by the bar. *B*, same traces as illustrated in *A* but with the glutamate-evoked current recorded in the absence of Mg^{2+} at −60 mV and −40 mV scaled to equal the steady-state current recorded at −80 mV. The extent of the inhibition decreases at more depolarized membrane potentials. *C*, TEVC traces recorded from an oocyte expressing NR1/NR2A NMDARs and voltage-clamped at either −80 mV or −40 mV. The black bar at the top of the trace in this panel and panels *D* and *E* below indicates the duration of the bath application of glutamate (3 μM), while the shaded bar in this panel (and those below) indicates the coapplication of Mg^{2+}. Increasing concentrations of Mg^{2+} were applied, cumulatively, as indicated by the arrowheads. *D*, TEVC traces recorded from an oocyte expressing NR1/NR2D NMDARs and voltage-clamped at either −80 mV or −40 mV illustrating the block of the glutamate-evoked current by increasing concentrations of Mg^{2+}. Note that NR1/NR2D NMDAR-mediated currents are less sensitive to block by Mg^{2+} compared to responses mediated by NR1/NR2A NMDARs. *E*, TEVC traces recorded from an oocyte expressing NR1/NR2A(2D-S1S2) NMDARs and voltage-clamped at either −80 mV or −40 mV illustrating the block of the glutamate-evoked current by increasing concentrations of Mg^{2+}. Note that NR1/NR2A(2D-S1S2) NMDAR-mediated currents are more sensitive to block by Mg^{2+} compared to responses mediated by NR1/NR2A NMDARs.

responses by 50% (IC_{50}) we constructed inhibition curves by applying increasing concentrations of Mg^{2+} to glutamate- and homoquinolinate-evoked currents. Figure 2*C*–*E* shows a series of TEVC traces recorded at −80 and −40 mV for NR1/NR2A (Fig. 2*C*), NR1/NR2D (Fig. 2*D*) and NR1/NR2A(2D-S1S2) (Fig. 2*E*) NMDARs and the inhibition of these responses by increasing concentrations of Mg^{2+} (3 μM to 10 mM). From the traces illustrated it is apparent that NR1/NR2D NMDAR-mediated responses are inhibited to a lesser extent (at equivalent concentrations of Mg^{2+}) than responses mediated by NR1/NR2A NMDARs. This finding is in agreement with previously published data (Monyer *et al.* 1992; Kuner & Schoepfer, 1996; Qian *et al.* 2005). However, responses mediated by the chimeric NMDAR construct, NR1/NR2A(2D-S1S2), are more potently inhibited by Mg^{2+} compared to responses mediated by wild-type NR2A-containing NMDARs.

Figure 3 shows the mean inhibition curves obtained for Mg^{2+} block of glutamate-evoked responses at each of the NMDAR constructs investigated in this study. Figure 4 shows the equivalent data for inhibition by Mg^{2+} of homoquinolinate-evoked responses at wild-type and chimeric NMDARs. Table 1 gives the mean IC_{50} values for each receptor combination at the three holding potentials we have investigated; for the inhibition of glutamate-evoked NR1/NR2A and NR1/NR2D NMDAR-mediated responses, the values are in good agreement with previously published studies examining these two NMDAR subtypes (Wyllie *et al.* 1996; Qian *et al.* 2005).

Aside from the clear dependence of the IC_{50} values on the holding potential for each construct, we can see that for both glutamate- and homoquinolinate-evoked responses, Mg^{2+} potency at NR2A-containing NMDARs is greater (lower IC_{50} values) than that seen at NR2D-containing

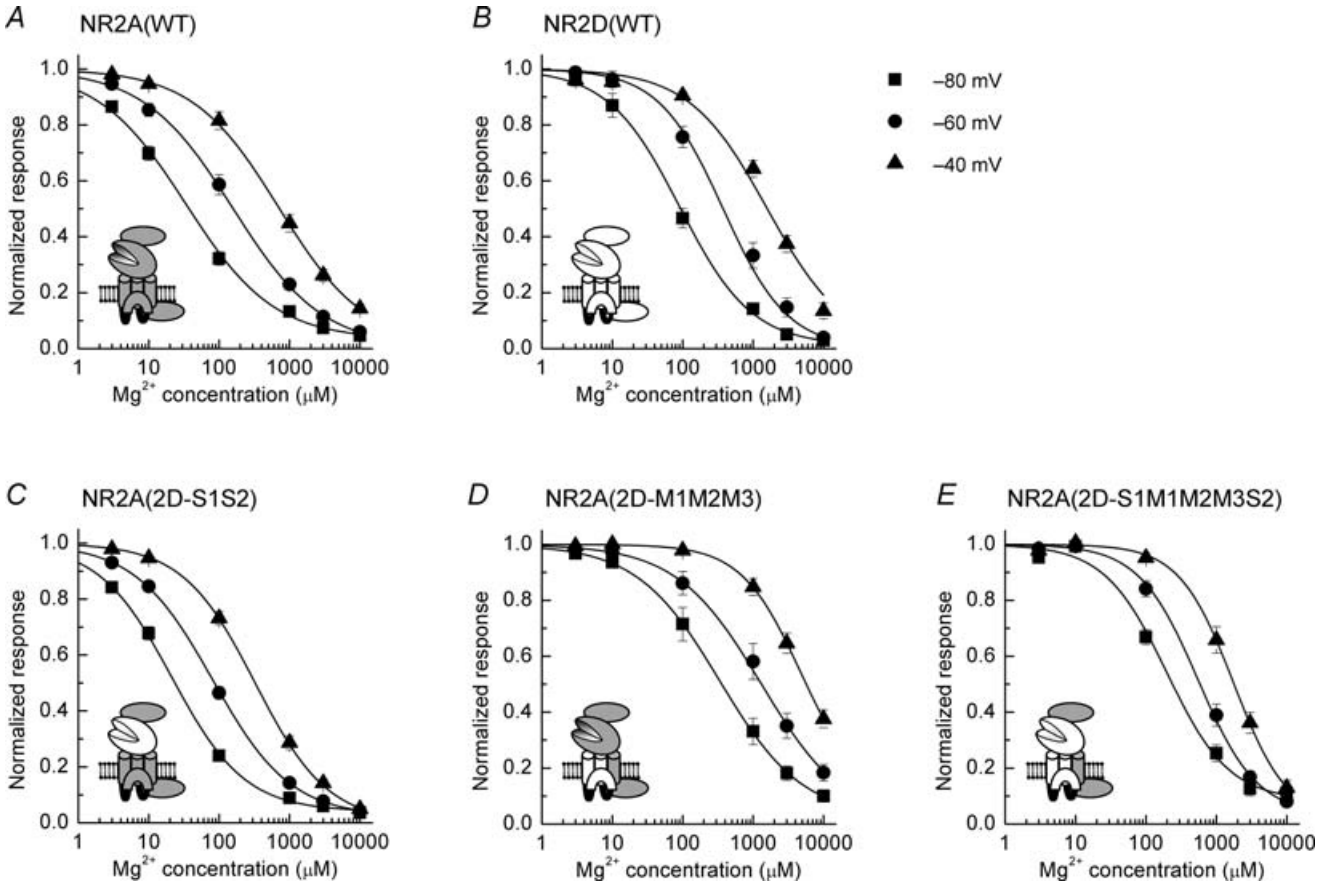

Figure 3. Mean inhibition curves for Mg^{2+} block of glutamate-evoked currents mediated by wild-type and chimeric NMDARs

A, mean inhibition curves for Mg^{2+} block of glutamate-evoked NR1/NR2A NMDAR-mediated currents. Inhibition curves were constructed at −80 mV (■), −60 mV (●) and −40 mV (▲) and fitted with the Hill equation (see Methods). *B*, mean inhibition curves for Mg^{2+} block of NR1/NR2D NMDAR-mediated currents. *C*, mean inhibition curves for Mg^{2+} block of NR1/NR2A(2D-S1S2) NMDAR-mediated currents. *D*, mean inhibition curves for Mg^{2+} block of NR1/NR2A(2D-M1M2M3) NMDAR-mediated currents. *E*, mean inhibition curves for Mg^{2+} block of NR1/NR2A(2D-S1M1M2M3S2) NMDAR-mediated currents. Mean IC_{50} values determined at each holding potential for each construct are given in Table 1.

NMDARs (Figs 3*A* and *B*, and 4*A* and *B*). As is suggested from the TEVC traces shown in Fig. 2, inclusion of the NR2D subunit LBD in NR2A subunits results in an approximately 2-fold increase in Mg^{2+} potency at each of the holding potentials examined ($P < 0.05$; Figs 3*C* and 4*C*). As the potency of glutamate acting at NR1/NR2A(2D-S1S2) NMDARs is greater than that seen at NR1/NR2A NMDARs (Erreger *et al.* 2007) we confirmed that the increase in Mg^{2+} potency seen at NR2A(2D-S1S2)-containing NMDARs was not the result of determining IC_{50} values at equivalent, but non-equipotent, glutamate concentrations (3 μM; equivalent to the EC_{50} for NR1/NR2A NMDARs). Thus, we determined IC_{50} values for Mg^{2+} using a glutamate concentration equal to its EC_{50} value at this construct (500 nM; Erreger *et al.* 2007). Mean IC_{50} values for Mg^{2+} when this lower concentration of glutamate was used were 13 ± 1 μM (−80 mV, $n = 7$), 72 ± 11 μM (−60 mV, $n = 8$) and 340 ± 54 μM (−40 mV, $n = 7$). These values (at a given holding potential) are not significantly different from those obtained when glutamate was used at the higher concentration (3 μM; $P > 0.05$, for each two-tailed *t* test). Inclusion of the M1M2M3 region of the NR2D subunit in NR2A subunits results in a rightward-shift in the inhibition curves for both glutamate- and homoquinolinate-evoked responses (decrease in Mg^{2+} potency) compared to NR1/NR2A NMDARs (Figs 3*D* and 4*D*). Given that this region contains key elements that determine Mg^{2+} potency (Kuner & Schoepfer, 1996; Wollmuth *et al.* 1998) a reduction in potency is to be expected although the extent of the shift is greater than that seen when comparing wild-type NR2A- and NR2D-containing NMDARs. However, when the S1S2 region from NR2D was included together with the

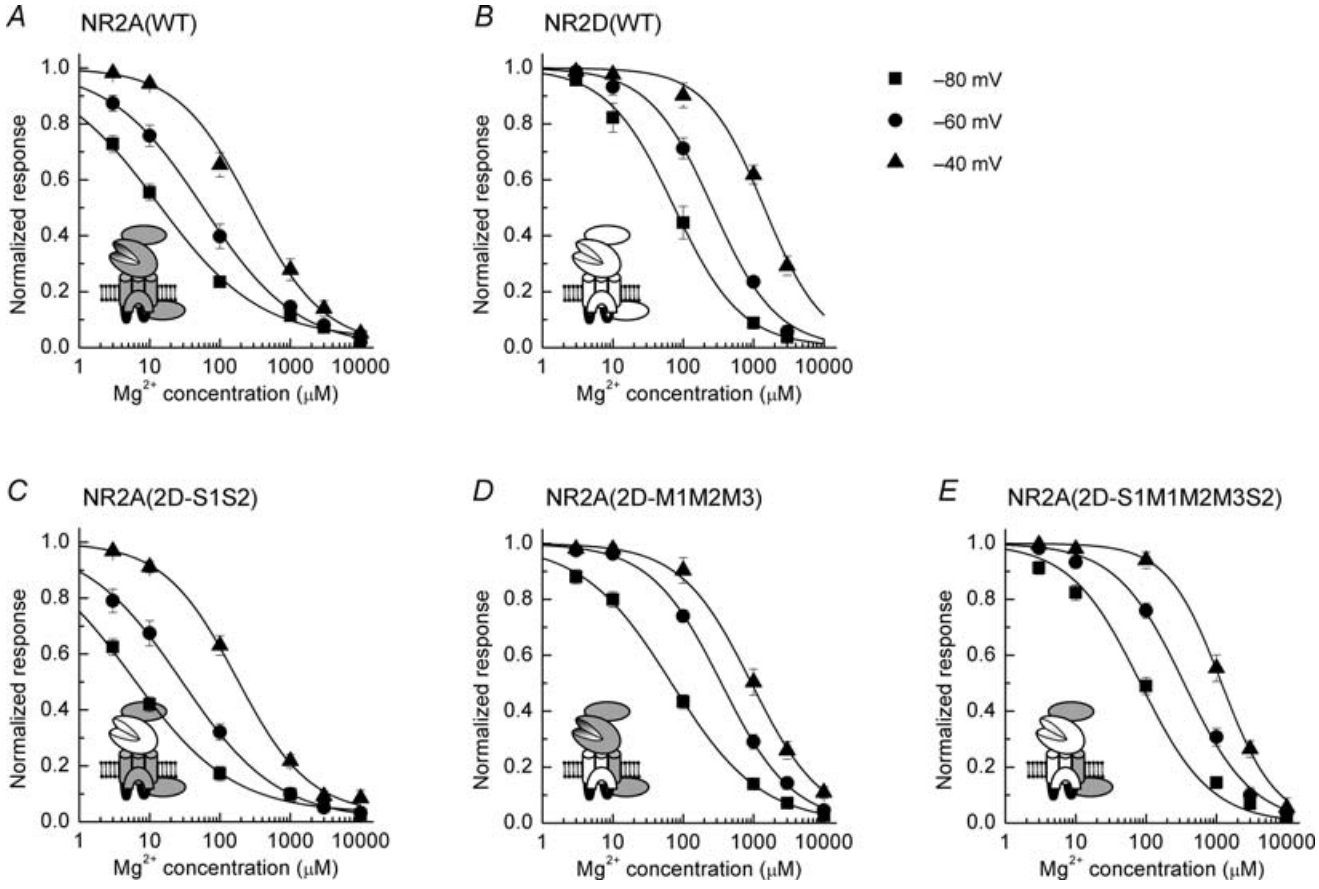

Figure 4. Mean inhibition curves for Mg^{2+} block of homoquinolinate-evoked currents mediated by wild-type and chimeric NMDARs

A, mean inhibition curves for Mg^{2+} block of homoquinolinate-evoked NR1/NR2A NMDAR-mediated currents. Inhibition curves were constructed at −80 mV (■), −60 mV (●) and −40 mV (▲) and fitted with the Hill equation (see Methods). *B*, mean inhibition curves for Mg^{2+} block of NR1/NR2D NMDAR-mediated currents. *C*, mean inhibition curves for Mg^{2+} block of NR1/NR2A(2D-S1S2) NMDAR-mediated currents. *D*, mean inhibition curves for Mg^{2+} block of NR1/NR2A(2D-M1M2M3) NMDAR-mediated currents. *E*, mean inhibition curves for Mg^{2+} block of NR1/NR2A(2D-S1M1M2M3S2) NMDAR-mediated currents. Mean IC_{50} values determined at each holding potential for each construct are given in Table 1.

Table 1. IC_{50} concentrations of Mg^{2+} and memantine required to inhibit glutamate- or homoquinolinate-evoked currents

	$IC_{50(-80\ mV)}$	$IC_{50(-60\ mV)}$	$IC_{50(-40\ mV)}$
Mg^{2+}, glutamate			
NR2A(WT)	34 ± 4 μM (15)	157 ± 24 μM (15)	701 ± 84 μM (15)
NR2D(WT)	91 ± 13 μM (13)	375 ± 52 μM (13)	1.6 ± 0.1 mM (13)
NR2A(2D-S1S2)	19 ± 1 μM (32)	78 ± 6 μM (32)	335 ± 21 μM (31)
NR2A(2D-M1M2M3)	335 ± 27 μM (11)	1.3 ± 0.2 mM (11)	4.7 ± 0.5 mM (11)
NR2A(2D-S1M1M2M3S2)	197 ± 31 μM (15)	548 ± 90 μM (15)	1.7 ± 0.4 mM (15)
Mg^{2+}, homoquinolinate			
NR2A(WT)	13 ± 2 μM (18)	58 ± 9 μM (17)	277 ± 57 μM (16)
NR2D(WT)	74 ± 16 μM (8)	263 ± 29 μM (9)	1.4 ± 0.1 mM (10)
NR2A(2D-S1S2)	5.7 ± 0.8 μM (16)	28 ± 5 μM (15)	172 ± 33 μM (14)
NR2A(2D-M1M2M3)	68 ± 7 μM (15)	349 ± 26 μM (15)	934 ± 123 μM (12)
NR2A(2D-S1M1M2M3S2)	83 ± 6 μM (13)	346 ± 37 μM (18)	1.2 ± 0.1 mM (14)
Memantine, glutamate			
NR2A(WT)	0.86 ± 0.08 μM (12)	1.7 ± 0.2 μM (11)	3.2 ± 0.5 μM (9)
NR2D(WT)	0.29 ± 0.04 μM (6)	0.42 ± 0.03 μM (6)	0.74 ± 0.06 μM (6)
NR2A(2D-S1S2)	1.0 ± 0.09 μM (8)	1.6 ± 0.2 μM (6)	2.3 ± 0.3 μM (6)
NR2A(2D-M1M2M3)	0.76 ± 0.09 μM (6)	1.5 ± 0.1 μM (6)	2.0 ± 0.2 μM (6)
NR2A(2D-S1M1M2M3S2)	0.83 ± 0.08 μM (6)	1.6 ± 0.2 μM (6)	2.7 ± 0.7 μM (6)

Values are given as means, with the errors taken from the standard error estimated from the non-linear curve fit of the data to eqn (1). Numbers in parentheses indicate the number of oocytes studied.

M1M2M3 region this resulted in a reduction in Mg^{2+} IC_{50} values for the inhibition of glutamate-evoked currents, compared to the values determined for the chimera containing the NR2D M1M2M3 region alone (Fig. 3*E*). This is analogous to the effect seen when the NR2D S1S2 region replaced the corresponding region in NR2A subunits. This effect of the NR2D S1S2 region in increasing Mg^{2+} potency at NMDARs containing NR2A subunits with the NR2D M1M2M3 region, however, was not seen when currents were evoked by homoquinolinate (Fig. 4*E*).

Another feature of the calculated IC_{50} values is the fact that Mg^{2+} more potently inhibits currents mediated by NR1/NR2A NMDARs evoked by homoquinolinate (10 μM) than those evoked by glutamate. We confirmed that using homoquinolinate at its EC_{50} (25 μM; Erreger *et al.* 2005) value also gave IC_{50} values for Mg^{2+} that were similarly more potent that those obtained when the equipotent concentration of glutamate (3 μM) evoked responses at this receptor combination. Mean IC_{50} values for Mg^{2+} when homoquinolinate at its EC_{50} concentration was used were 12 ± 3 μM (−80 mV, $n = 8$), 42 ± 15 μM (−60 mV, $n = 8$) and 155 ± 58 μM (−40 mV, $n = 8$). These IC_{50} values (at a given holding potential) are not significantly different from those obtained with the lower (10 μM) concentration of homoquinolinate ($P > 0.1$; for each two-tailed t test). This effect of homoquinolinate on increasing Mg^{2+} block is not observed at NR1/NR2D NMDARs where the IC_{50} values of glutamate- and homoquinolinate-evoked responses are not significantly different.

Voltage-dependent block of glutamate-evoked currents by memantine

Memantine is another example of an NMDAR channel blocker; however, unlike Mg^{2+} its potency at NR1/NR2D NMDARs is greater than that at NR1/NR2A NMDARs (Parsons *et al.* 1999*a*; Dravid *et al.* 2007). Figure 5 shows a series of TEVC traces illustrating features of the block of NMDAR-mediated currents by memantine. Memantine, like Mg^{2+}, is a reversible blocker of NMDAR-mediated currents. Figure 5*A* shows a typical response from an oocyte expressing NR1/NR2A NMDARs following application of glutamate (3 μM). Addition of memantine (100 nM) reduces the magnitude of the current recorded and increasing the concentration (10 μM) of this blocker results in further inhibition of the response. When the concentration of memantine is reduced, the response recovers to the level seen when the blocker was applied for the first time. Thus, the reversibility and recovery of responses allows us to construct cumulative inhibition curves to determine IC_{50} values for this channel blocker. Figure 5*B* shows the effect of increasing concentrations of memantine (10 nM to 100 μM) on a glutamate-evoked NR1/NR2A NMDAR-mediated current recorded at −80 and −40 mV. Figure 5*C* shows corresponding TEVC traces obtained from an oocyte expressing NR1/NR2D NMDARs. These traces illustrate (and in agreement with previous work) that memantine is more potent at blocking NR1/NR2D NMDAR-mediated responses than those mediated by NR1/NR2A NMDARs (Parsons *et al.* 1999*a*). Figure 6 shows the mean inhibition curves obtained for

memantine block of glutamate-evoked responses at each of the NMDAR constructs investigated in this study, while the mean IC_{50} values obtained from the analysis of this dataset are given in Table 1. Inspection of the IC_{50} values indicates that memantine is a more potent blocker of NMDAR-mediated response for each of the receptor constructs examined. As is the case with Mg^{2+} block, the extent of memantine block decreases as the membrane potential is voltage-clamped at more depolarized levels. However, the relative shift in IC_{50} values is less than that observed for Mg^{2+} block of currents mediated by the same NMDAR construct (see below). While memantine was significantly ($P < 0.01$) more potent at NR2D-containing NMDARs compared with their NR2A-containing counterparts at all potentials examined, in contrast with our observations concerning Mg^{2+} block described above, none of the chimeric NMDAR constructs displayed significant differences in their IC_{50} values compared to the parent NR2A-containing NMDARs ($P > 0.05$).

Current–voltage plots of NMDAR-mediated currents in the presence of Mg^{2+} and memantine and voltage dependence of block

For each of the NMDAR constructs characterized in this study we generated current–voltage plots in the absence and presence of either Mg^{2+} (1 mM) or memantine (10 μM) and the mean plots are illustrated in the online supplemental material, Supplemental Fig. 1. As is to be expected, each of the NMDAR constructs shows a linear current–voltage relationship in the absence of blocker. A small amount of rectification is apparent in the plot for NR2A(2D-S1S2)-containing NMDARs (Supplemental Fig. 1*C*) perhaps reflecting the fact that these receptor–channels are the most sensitive to block by Mg^{2+} and the presence of small amounts of 'contaminating' Mg^{2+} from our salt solutions may lead to deviations from linearity at hyperpolarized membrane potentials. Each NMDAR construct gave a current–voltage plot, in the presence of Mg^{2+}, with a

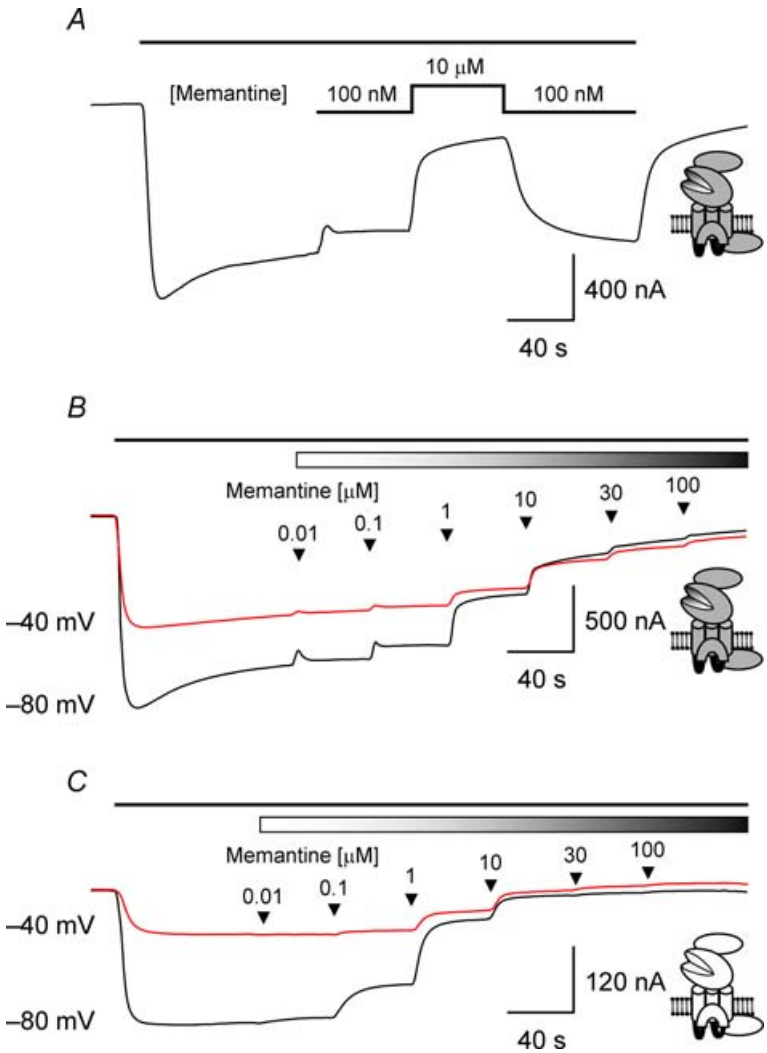

Figure 5. TEVC current recordings illustrating block by memantine of glutamate-evoked responses mediated by NR2A- and NR2D-containing NMDARs
A, TEVC trace recorded from an oocyte expressing NR1/NR2A NMDARs and voltage-clamped at −80 mV. The black bar at the top of the trace in this panel and panels *B* and *C* below indicates the duration of the bath application of glutamate (3 μM). The reversibility of memantine block is illustrated by coapplying with glutamate, memantine at two concentrations (100 nM or 10 μM). Switching the memantine concentration from 10 μM to 100 nM results in a recovery of the glutamate-evoked current to the level seen when memantine was first applied. *B*, TEVC traces recorded from an oocyte expressing NR1/NR2A NMDARs and voltage-clamped at either −80 mV or −40 mV. The shaded bar in this panel (and in panel *C* below) indicates the coapplication memantine. Increasing concentrations of memantine were applied, cumulatively, as indicated by the arrowheads. *C*, TEVC traces recorded from an oocyte expressing NR1/NR2D NMDARs and voltage-clamped at either −80 mV or −40 mV illustrating the block of the glutamate-evoked current by increasing concentrations of memantine. Note that NR1/NR2D NMDAR-mediated currents are more sensitive to block by memantine compared to responses mediated by NR1/NR2A NMDARs.

typical J-shaped profile. As would be expected from the IC_{50} values described above, the current–voltage plot for NR2A(2D-S1S2)-containing NMDARs showed the greatest levels of inhibition, while the least inhibition was seen with NR2A(2D-M1M2M3)-containing NMDARs (Supplemental Fig. 1*C* and *D*, respectively). In contrast to the current–voltage plots for Mg^{2+}, those for memantine displayed less-pronounced regions of 'negative slope conductance' with the overall profile of the current–voltage plot being similar to that described for native NMDARs (Parsons *et al.* 1993).

We compared the voltage dependence of Mg^{2+} and memantine block by plotting the measured IC_{50} values against the membrane potential at which they had been determined (Fig. 7). For each NMDAR construct examined, the fitted line describing the voltage dependence of memantine block is shallower than that describing Mg^{2+} block of NMDAR-mediated responses. This decreased slope corresponds to lower estimates of δ (the fraction of the electric field experienced by the blocker) for memantine block compared to Mg^{2+} block of the corresponding NMDAR-mediated current. Comparison of the mean δ values for the inhibition by Mg^{2+} of glutamate- and homoquinolinate-evoked currents and for the inhibition by memantine of glutamate-evoked currents is illustrated in Fig. 7*F*–*H*. Overall, δ values for memantine are less than those for Mg^{2+} at each of the constructs studied confirming the weaker voltage dependence of memantine block.

Discussion

Comparisons of NR2A- and NR2D-containing NMDARs have shown that, in general, these two NMDAR

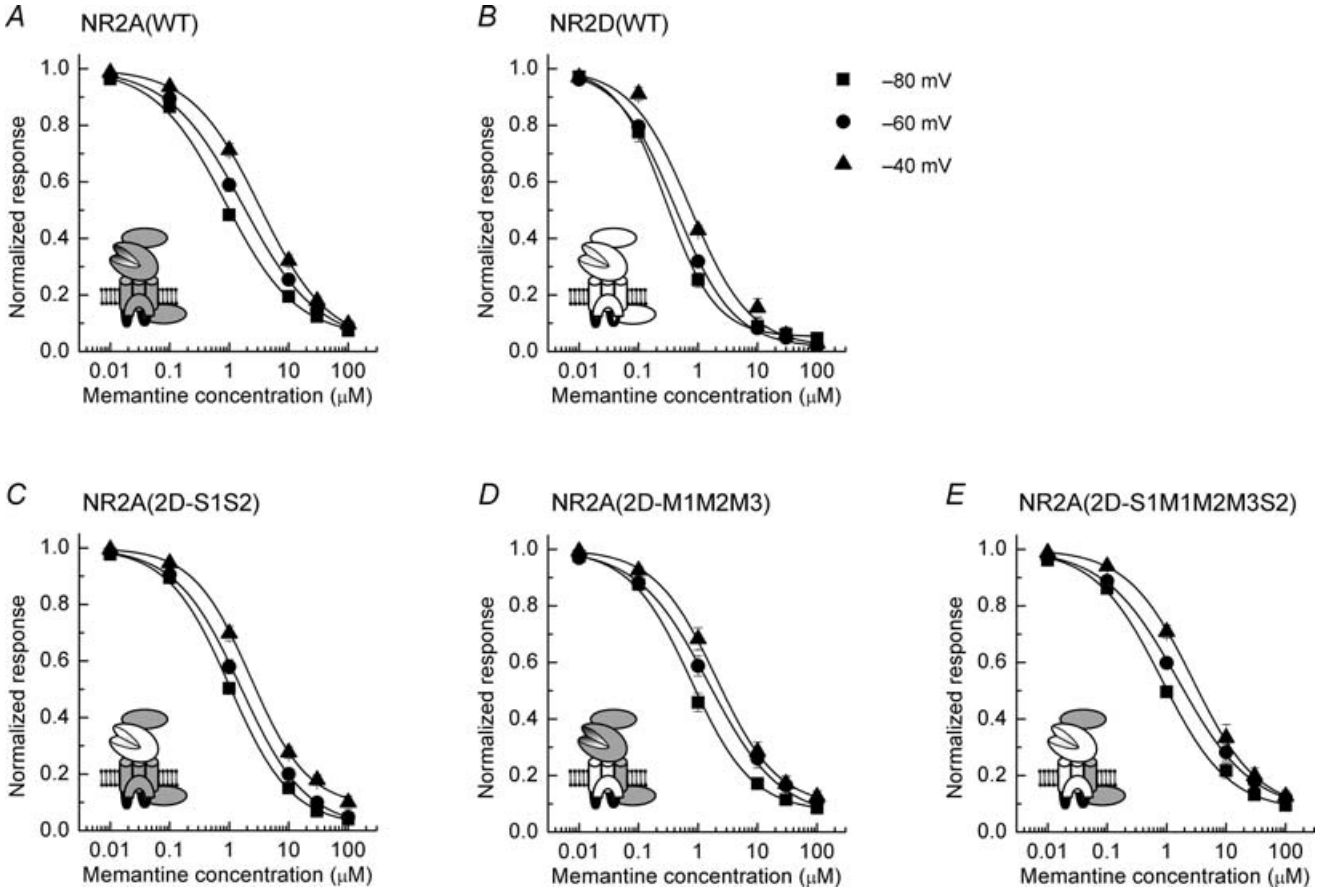

Figure 6. Mean inhibition curves for memantine block of glutamate-evoked currents mediated by wild-type and chimeric NMDARs

A, mean inhibition curves for memantine block of glutamate-evoked NR1/NR2A NMDAR-mediated currents. Inhibition curves were constructed at −80 mV (■), −60 mV (●) and −40 mV (▲) and fitted with the Hill equation (see Methods). *B*, mean inhibition curves for Mg^{2+} block of NR1/NR2D NMDAR-mediated currents. *C*, mean inhibition curves for Mg^{2+} block of NR1/NR2A(2D-S1S2) NMDAR-mediated currents. *D*, mean inhibition curves for Mg^{2+} block of NR1/NR2A(2D-M1M2M3) NMDAR-mediated currents. *E*, mean inhibition curves for Mg^{2+} block of NR1/NR2A(2D-S1M1M2M3S2) NMDAR-mediated currents. Mean IC_{50} values determined at each holding potential for each construct are given in Table 1.

subtypes show the greatest differences in their biophysical and pharmacological properties (for example see Monyer *et al.* 1992, 1994; Kuner & Schoepfer, 1996; Wyllie *et al.* 1996, 1998; Buller & Monaghan, 1997; Vicini *et al.* 1998; Parsons *et al.* 1999*a*; Qian *et al.* 2005; Erreger *et al.* 2007). Indeed such differences have been exploited to identify unambiguously NR2D-containing NMDARs in native neurones (Momiyama *et al.* 1996; Misra *et al.* 2000*a*,*b*; Brickley *et al.* 2003). In this present study, in addition to characterizing the channel block produced by Mg^{2+} and memantine at these two NMDAR subtypes, we have adopted the strategy of creating chimeric receptors to allow us to probe how the 'functional domains' within these NMDAR subtypes influence the actions of these two channel blockers. Notwithstanding the differences in the sensitivities of NR2A- and NR2D-containing NMDARs to the two channel blockers investigated here, three well-characterized differences in NR1/NR2A and NR1/NR2D NMDAR properties are (1) the fact that most NMDAR agonists are considerably more potent at NR2D- than NR2A-containing NMDARs (Erreger *et al.* 2007), (2) the very slow deactivation of NR2D-containing NMDARs compared with the more rapid deactivation of NR2A-containing NMDARs (Monyer *et al.* 1992, 1994; Vicini *et al.* 1998; Wyllie *et al.* 1998), and (3) the lower single-channel conductance and transition asymmetry of NR2D- compared to NR2A-containing NMDARs (Wyllie *et al.* 1996, 1998). Given that the potency with which an agonist interacts with its receptor will influence (but not completely determine) the deactivation of its

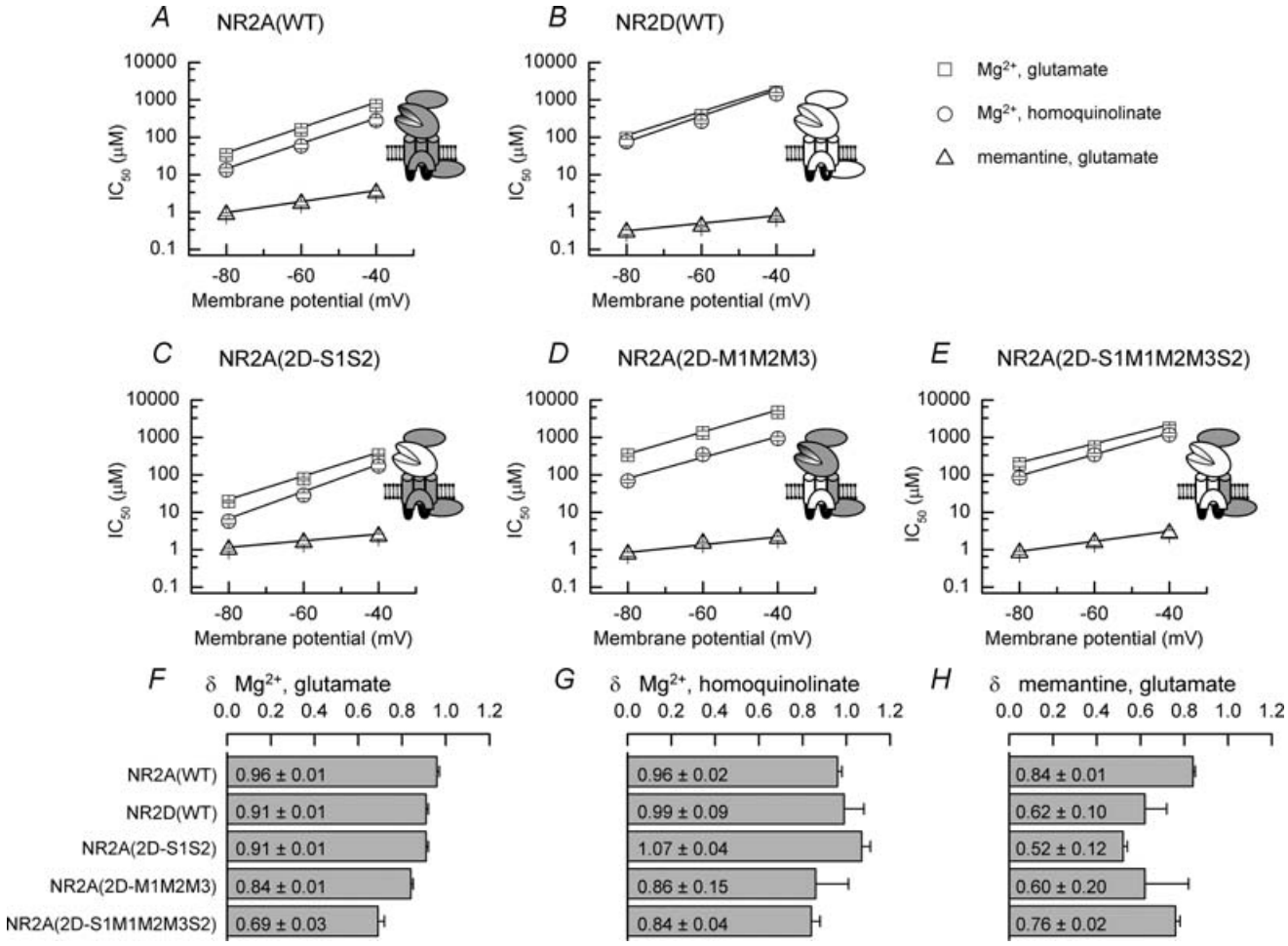

Figure 7. Voltage dependence of IC_{50} values for Mg^{2+} and memantine block of wild-type and chimeric NMDAR-mediated responses and comparison of δ values

A–E, plots of the voltage dependence of the mean IC_{50} value for Mg^{2+} block of glutamate-evoked (□) or homoquinolinate-evoked (○) currents and memantine block of glutamate-evoked currents (△) in oocytes expressing NR1/NR2A NMDARs (*A*), NR1/NR2D NMDARs (*B*), NR1/NR2A(2D-S1S2) NMDARs (*C*), NR1/NR2A(2D-M1M2M3) NMDARs (*D*) or NR1/NR2A(2DS1M1M2M3S2) NMDARs (*E*). Note that for each plot the slope of the line describing memantine block of the currents is shallower than that seen for Mg^{2+} block of the same NMDAR-mediated current, though the potency of memantine is greater than that of Mg^{2+}. *F–H*, bar graphs showing δ values determined from analysis of Mg^{2+} block of glutamate-evoked currents (*F*), Mg^{2+} block of homoquinolinate-evoked currents (*G*) and memantine block of glutamate-evoked currents (*H*). Mean δ values for each of the blockers are indicated.

response and similarly factors that influence channel gating are contained (although not exclusively) within pore-forming regions of the receptor led us to determine to what extent the LBD ('potency-determining') and the M1M2M3 ('gating-determining') membrane-associated regions influenced the channel block produced by Mg^{2+} and memantine. In addition by using homoquinolinate (a partial agonist at NR2A-containing receptors) we could determine whether the nature of the ligand–binding–gating interaction also had an impact on the potency of channel block.

Mg^{2+} block of wild-type and chimeric NMDARs

In agreement with previous studies (Monyer *et al.* 1992, 1994; Kuner & Schoepfer, 1996; Qian *et al.* 2005) we find that Mg^{2+} is a more potent blocker of NR2A- compared with NR2D-containing NMDARs. In addition, we also observed a lack of dependence of IC_{50} for Mg^{2+} block on the agonist concentration used. Such a result is also consistent with the observation that Mg^{2+} itself does not alter channel gating in the sense that the durations of 'bursts' of channel openings do not change in the presence of Mg^{2+} (Ascher & Nowak, 1988). However, while we checked that the IC_{50} values we obtained were independent of the agonist concentration used, differences in the individual single-channel P_{open} values between NR1/NR2A and NR1/NR2D NMDARs (Wyllie *et al.* 1998) are also likely to influence the ability of Mg^{2+} to block these receptor subtypes. The values we determined for the IC_{50} for Mg^{2+} block of both wild-type NMDARs are in good agreement with a previously published study (Qian *et al.* 2005) but are somewhat higher (implying lower Mg^{2+} potency in our study) than other studies that have expressed recombinant NMDARs in oocytes (for example Kawajiri & Dingledine, 1993; Sakurada *et al.* 1993; Kuner & Schoepfer, 1996; Kupper *et al.* 1996). Indeed the large range of IC_{50} values that have been reported for NR1/NR2A and NR1/NR2D NMDARs has been highlighted previously (Qian *et al.* 2005). It remains unclear what factors might be responsible for these wide ranges; however, given that the nature of the permeant ions influences both the potency of Mg^{2+} block and estimates of δ values (Antonov & Johnson, 1999; Zhu & Auerbach, 2001*a*,*b*; Qian *et al.* 2002; Qian & Johnson, 2006) the use, in this study, of $BaCl_2$ (1.8 mM) in the external recording solution may contribute to the lower potency of Mg^{2+} we report here for wild-type NR2A- and NR2D-containing NMDARs. While there is therefore a wide-range of potencies that have been reported for block by Mg^{2+} of various NMDARs the experiments described here have been conducted using the same ionic composition of solutions and have made several additional findings concerning Mg^{2+} block of NMDARs that are discussed below.

Our data show that inclusion of the NR2D S1S2 region in the NR2A subunit leads to an increase in the potency with which Mg^{2+} inhibits both glutamate- and homoquinolinate-evoked responses. We confirmed that the ~2-fold increase in Mg^{2+} potency observed was not due to differences in agonist potencies at NR2A- and NR2A(2D-S1S2)-containing NMDARs which might influence the extent of Mg^{2+} block observed. We suggest that elements within the NR2D LBD linking ligand binding to channel gating interact differently compared to the NR2A LBD and this leads ultimately to a channel conformation that is more potently inhibited by Mg^{2+}. Nevertheless, such a conformation does not alter the fraction of the electric field experienced by Mg^{2+}. This indicates that while the binding potency of Mg^{2+} has been affected, the location of the block site in the pore remains constant (Fig. 7). It is interesting to note that a recent report (Gee *et al.* 2007) has provided evidence that the ability of functional domains out with pore-forming regions to influence channel properties may not be restricted to NMDARs. In their study of chimeric $5HT_{3A}$-α7 nicotinic acetylcholine receptors, inclusion of the α7 amino-terminal region in certain $5HT_{3A}$ receptor constructs resulted in a 3-fold increase in single-channel conductance. Thus in members of the nicotinic superfamily of ion channels, ligand-binding regions may also influence ion permeation and pore characteristics.

Intriguingly, homoquinolinate-evoked responses mediated by NR1/NR2A NMDARs are more potently inhibited by Mg^{2+} than responses evoked by glutamate. Again we ensured that this change in potency was not a consequence of using non-equivalent agonist concentrations by determining Mg^{2+} IC_{50} values at the respective EC_{50} concentrations of glutamate (3 μM) and homoquinolinate (25 μM). This effect of homoquinolinate was not observed at NR2D-containing NMDARs, at which, it is perhaps worth noting, it is a near full agonist and is also an example of one of the few ligands that does not show increased potency at NR2D- compared to NR2A-containing NMDARs (Erreger *et al.* 2007). It has been proposed that the nature of the interaction of homoquinolinate with its binding site in the NR2A subunit causes differences in the position of Helix F that may account for aspects of its partial agonist action (Erreger *et al.* 2005). Thus, while the present study does not identify how these interactions lead ultimately to a change in sensitivity to Mg^{2+} block they do support the notion that different agonists give rise to subtly different receptor–channel conformations.

Finally, NR1/NR2D NMDARs have been shown to have a faster apparent unblocking rate (k_{-app}) for Mg^{2+} relative to NMDARs containing NR2A subunits (Qian *et al.* 2005). Therefore since the NR1/NR2A(2D-M1M2M3) chimeric construct places a 'NR2D-like' pore region into an NR2A subunit it is perhaps not surprising that

we observed a considerably reduced Mg^{2+} potency at this chimera compared to NR2A-containing NMDARs. However, the extent of the shift (∼10-fold decrease) is greater than might be expected from the experimentally derived values for k_{-app} which display only around a 3-fold difference for NR2A- and NR2D-containing NMDARs (Qian *et al.* 2005). Indeed IC_{50} values for the NR1/NR2A(2D-M1M2M3) chimeric construct show that Mg^{2+} is less potent at this subunit combination than it is at NR2D-containing NMDARs. As an explanation as to why simply replacing the major part of the pore-forming region of NR2A subunits with that from NR2D subunits does not give an overall 'NR2D-like' Mg^{2+} sensitivity, we propose that the sensitivity of NR2D-containing NMDARs is influenced not only by the pore-forming regions, but also by a contribution from the NR2D LBD. Inclusion of both these structural elements in the chimera, NR2A(2D-S1M1M2M3S2), gives rise to an NMDAR that is more potently blocked by Mg^{2+} compared to the NR2A(2D-M1M2M3) chimera and also adds to the evidence that the nature of the LBD influences the properties of voltage-dependent Mg^{2+} block. In a previous study Kuner & Schoepfer (1996) demonstrated that an NR1/NR2B NMDAR sensitivity to Mg^{2+} ions could be reproduced in a chimeric NR1/NR2C NMDAR that contained the four membrane associated regions found in NR2B NMDAR subunits. Our study has not examined the role of M4 and therefore we cannot rule out the possibility that, as is the case for NR2B and NR2C NMDAR subunits, this region would influence Mg^{2+} potency in NR2A/2D chimeras. Nonetheless, our observations show that the nature of the LBD, and in the case of NR1/NR2A NMDARs, the nature of the ligand used, influences the potency of Mg^{2+} block. While the precise mechanism by which this occurs is unclear, we suggest that the different conformations adopted by the LBD and subsequent channel-gating are contributing factors.

Memantine block of wild-type and chimeric NMDARs

In agreement with previously published data (Parsons *et al.* 1999*a*; Chen & Lipton, 2005; Dravid *et al.* 2007), memantine is a potent blocker of NMDAR-mediated responses being more potent at NR2D-containing than NR2A-containing NMDARs. Indeed, our estimates of the IC_{50} for memantine block of NR1/NR2A and NR1/NR2D NMDARs are in excellent agreement with previously published values (Parsons *et al.* 1999*a*; Chen & Lipton, 2005; Dravid *et al.* 2007) and those observed for native NMDARs (Gilling *et al.* 2007). In addition, block by memantine is less voltage dependent than that seen with Mg^{2+}, as is indicated by the decreased slopes in the plots of IC_{50} *versus* membrane potential (Fig. 7). Our estimates of δ for memantine block are lower than the corresponding values for Mg^{2+} block, indicating that while there may be overlap in the binding sites for these two blockers, they are also distinct (Kashiwagi *et al.* 2002; Chen & Lipton, 2005). It is known that memantine binds to both a high- and low-affinity site in the NMDAR pore (Blanpied *et al.* 1997; Chen & Lipton, 2005) with the asparagine residue of the QRN-site in the M2 region of the NR1 NMDAR subunit being a major contributor to the high-affinity site. Since the NR1 subunit is common to, and not altered in, each of the wild-type and chimeric NMDARs we have studied, this might be a contributing factor to explain why we did not transfer 'NR2D-like' potency to NR2A subunits when they contained the NR2D M1M2M3 region. Moreover chimeras expressing the NR2D LBD did not influence the potency of memantine block. Therefore the contribution of the NR2D LBD in affecting Mg^{2+} potency does not extend to memantine. A recent study (Gilling *et al.* 2007) has demonstrated that the potency of memantine block at equilibrium is not affected by the agonist concentration used to activate the NMDA receptor–channel. This finding indicates that although glutamate potencies at the wild-type and chimeric NMDARs investigated in the present study vary, this is unlikely to influence the IC_{50} values we have obtained for each of the constructs. Thus, our data suggest that the elements that give rise to more potent block of NR2D-containing compared to NR2A-containing NMDARs by memantine are out with both the LBD and M1M2M3 regions.

Conclusion

Voltage-dependent channel block of NMDARs is one of the defining characteristics of this family of ligand-gated ion channels. While the major determinants of this block reside in the M2 region of both NR1 and NR2 NMDAR subunits, other elements contained within the M1 domain, M2–M3 linker and M4 domain also contribute to the potency of voltage-dependent block. Our data are consistent with this notion. Nevertheless, this study shows that in addition to these regions, the LBD of NMDARs also contributes to the potency of Mg^{2+} block. Thus, not only does the LBD of NMDARs determine agonist potency at these receptor–channels (Laube *et al.* 1997; Anson *et al.* 1998, 2000; Chen *et al.* 2004, 2005; Erreger *et al.* 2007) but it is emerging that this region also plays a role in influencing glycine (coagonist) potency (Chen *et al.* 2007) and voltage-dependent Mg^{2+} block.

References

Anson LC, Chen PE, Wyllie DJA, Colquhoun D & Schoepfer R (1998). Identification of amino acid residues of the NR2A subunit that control glutamate potency in recombinant NR1/NR2A NMDA receptors. *J Neurosci* **18**, 581–589.

Anson LC, Schoepfer R, Colquhoun D & Wyllie DJA (2000). Single-channel analysis of an NMDA receptor possessing a mutation in the region of the glutamate binding site. *J Physiol* **527**, 225–237.

Antonov SM & Johnson J (1999). Permeant ion regulation of *N*-methyl-D-aspartate receptor channel block by Mg^{2+}. *Proc Natl Acad Sci U S A* **96**, 14571–14576.

Ascher P & Nowak L (1988). The role of divalent cations in the *N*-methyl-D-aspartate responses of mouse central neurones in culture. *J Physiol* **399**, 247–266.

Blanpied TA, Boeckman FA, Aizenman E & Johnson JW (1997). Trapping channel block of NMDA-activated responses by amantadine and memantine. *J Neurophysiol* **77**, 309–323.

Bliss TVP & Collingridge GL (1993). A synaptic model of memory: long-term potentiation in the hippocampus. *Nature* **361**, 31–39.

Brickley SG, Misra C, Mok MH, Mishina M & Cull-Candy SG (2003). NR2B and NR2D subunits coassemble in cerebellar Golgi cells to form a distinct NMDA receptor subtype restricted to extrasynaptic sites. *J Neurosci* **23**, 4958–4966.

Buller AL & Monaghan DT (1997). Pharmacological heterogeneity of NMDA receptors: characterization of NR1a/NR2D heteromers expressed in Xenopus oocytes. *Eur J Pharmacol* **320**, 87–94.

Burnashev N, Schoepfer R, Monyer H, Ruppersberg JP, Gunter W, Seeburg PH & Sakmann B (1992). Control by asparagine residues of calcium permeability and magnesium blockade in the NMDA receptor. *Science* **257**, 1415–1419.

Chen PE, Geballe MT, Katz K, Erreger K, Livesey MR, O'Toole KK, Le P, Lee CJ, Snyder JP, Traynelis SF & Wyllie DJA (2008). Allosteric modulation of glycine potency in rat recombinant NMDA receptors containing chimeric NR2A/2D subunits expressed in *Xenopus laevis* oocytes. *J Physiol* **586**, 227–245.

Chen PE, Geballe MT, Stansfeld PJ, Johnston AR, Yuan H, Jacob AL, Snyder JP, Traynelis SF & Wyllie DJA (2005). Structural features of the glutamate binding site in recombinant NR1/NR2A N-methyl-D-aspartate receptors determined by site-directed mutagenesis and molecular modeling. *Mol Pharmacol* **67**, 1470–1484.

Chen PE, Johnston AR, Mok MH, Schoepfer R & Wyllie DJA (2004). Influence of a threonine residue in the S2 ligand binding domain in determining agonist potency and deactivation rate of recombinant NR1/NR2D NMDA receptors. *J Physiol* **558**, 45–58.

Chen HSV & Lipton SA (2005). Pharmacological implications of two distinct mechanisms of interaction of memantine with *N*-methyl-D-aspartate-gated channels. *J Pharmacol Exp Ther* **314**, 961–971.

Chen PE & Wyllie DJA (2006). Pharmacological insights obtained from structure-function studies of ionotropic glutamate receptors. *Br J Pharmacol* **147**, 839–853.

Cull-Candy SG, Brickley S & Farrant M (2001). NMDA receptor subunits: diversity, development and disease. *Curr Opin Neurobiol* **11**, 327–335.

Dingledine R, Borges K, Bowie D & Traynelis SF (1999). The glutamate receptor ion channels. *Pharmacol Rev* **51**, 7–61.

Dravid SM, Erreger K, Yuan H, Nicholson K, Le P, Lyuboslavsky P, Almonte A, Murray E, Mosely C, Barber J, French A, Balster R, Murray TF & Traynelis SF (2007). Subunit-specific mechanisms and proton sensitivity of NMDA receptor channel block. *J Physiol* **581**, 107–128.

Erreger K, Chen PE, Wyllie DJA & Traynelis SF (2004). Glutamate receptor gating. *Crit Rev Neurobiol* **16**, 187–224.

Erreger K, Geballe MT, Dravid SM, Snyder JP, Wyllie DJA & Traynelis SF (2005). Mechanism of partial agonism at NMDA receptors for a conformationally restricted glutamate analog. *J Neurosci* **25**, 7858–7866.

Erreger K, Geballe MT, Kristensen A, Chen PE, Hansen KB, Lee CJ, Yuan H, Le P, Lyuboslavsky PN, Micale N, Jørgensen L, Clausen RP, Wyllie DJA, Snyder JP & Traynelis SF (2007). Subunit-specific agonist activity at NR2A, NR2B, NR2C, and NR2D containing *N*-methyl-D-aspartate glutamate receptors. *Mol Pharmacol* **72**, 907–920.

Frizelle PA, Chen PE & Wyllie DJA (2006). Equilibrium constants for (*R*)-[(*S*)-1-(4-bromo-phenyl)-ethylamino]-(2,3-dioxo-1,2,3,4-tetrahydroquinoxalin-5-yl)-methyl]-phosphonic acid (NVP-AAM077) acting at recombinant NR1/NR2A and NR1/NR2B NMDA receptors: implications for studies of synaptic transmission. *Mol Pharmacol* **70**, 1022–1032.

Gee VJ, Kracun S, Cooper ST, Gibb AJ & Millar NS (2007). Identification of domains influencing assembly and ion channel properties in $\alpha 7$ nicotinic receptor and 5-HT_3 receptor subunit chimaeras. *Br J Pharmacol* **152**, 501–512.

Gilling KE, Jatzke C & Parsons CG (2007). Agonist concentration dependency of blocking kinetics but not equilibrium block of *N*-methyl-D-aspartate receptors by memantine. *Neuropharmacology* **53**, 421–430.

Hollmann M, Boulter J, Maron C, Beasley L, Sullivan J, Pecht G & Heinemann S (1993). Zinc potentiates agonist-induced currents at certain splice variants of the NMDA receptor. *Neuron* **10**, 943–954.

Ishii T, Moriyoshi K, Sugihara H, Sakurada K, Kadotani H, Yokoi M, Akazawa C, Shigemoto R, Mizuno N & Masu M (1993). Molecular characterisation of the family of the *N*-methyl-D-aspartate receptor subunits. *J Biol Chem* **268**, 2836–2843.

Kashiwagi K, Masuko T, Nguyen CD, Kuno T, Tanaka I, Igarashi K & Williams K (2002). Channel blockers acting at *N*-methyl-D-aspartate receptors: differential effects of mutations in the vestibule and ion channel pore. *Mol Pharmacol* **61**, 533–545.

Kato N & Yoshimura H (1993). Reduced Mg^{2+} block of *N*-methyl-D-aspartate receptor-mediated synaptic potentials in developing visual cortex. *Proc Natl Acad Sci U S A* **90**, 7114–7118.

Kawajiri S & Dingledine R (1993). Multiple structural determinants of voltage-dependent magnesium block in recombinant NMDA receptors. *Neuropharmacology* **32**, 1203–1211.

Kleckner NW & Dingledine R (1991). Regulation of NMDA receptors by glycine and magnesium during development. *Mol Brain Res* **11**, 151–159.

Kuner T & Schoepfer R (1996). Multiple structural elements determine subunit specificity of Mg^{2+} block in NMDA receptor channels. *J Neurosci* **16**, 3549–3558.

Kupper J, Ascher P & Neyton J (1996). Probing the pore region of recombinant *N*-methyl-D-aspartate channels using external and internal magnesium block. *Proc Natl Acad Sci U S A* **93**, 8648–8653.

Laube B, Hirai H, Sturgess M, Betz H & Kuhse J (1997). Molecular determinants of agonist discrimination by NMDA receptor subunits: analysis of the glutamate binding site on the NR2B subunit. *Neuron* **18**, 493–503.

Lipton SA (2006). Paradigm shift in neuroprotection by NMDA receptor blockade: memantine and beyond. *Nat Rev Drug Discov* **5**, 160–170.

Mayer ML (2006). Glutamate receptors at atomic resolution. *Nature* **440**, 456–462.

Mayer ML & Armstrong N (2004). Structure and function of glutamate receptor ion channels. *Annu Rev Physiol* **66**, 161–181.

Mayer ML, Westbrook GL & Guthrie PB (1984). Voltage-dependent block by Mg^{2+} of NMDA responses in spinal cord neurons. *Nature* **309**, 261–263.

Misra C, Brickley SG, Farrant M & Cull-Candy SG (2000*a*). Identification of subunits contributing to synaptic and extrasynaptic NMDA receptors in Golgi cells of the rat cerebellum. *J Physiol* **524**, 147–162.

Misra C, Brickley SG, Wyllie DJA & Cull-Candy SG (2000*b*). Slow deactivation kinetics of NMDA receptors containing NR1 and NR2D subunits in rat cerebellar Purkinje cells. *J Physiol* **525**, 299–305.

Momiyama A, Feldmeyer D & Cull-Candy SG (1996). Identification of a native low-conductance NMDA channel with reduced sensitivity to Mg^{2+} in rat central neurones. *J Physiol* **494**, 479–492.

Monyer H, Burnashev N, Laurie DJ, Sakmann B & Seeburg PH (1994). Developmental and regional expression in the rat brain and function properties of four NMDA receptors. *Neuron* **12**, 529–540.

Monyer H, Sprengel R, Schoepfer R, Herb A, Higughi M, Lomeli H, Burnashev N, Sakmann B & Seeburg PH (1992). Heteromeric NMDA receptors: Molecular and functional distinctions of subtypes. *Science* **256**, 1217–1221.

Mori H, Masaki H, Yamakura T & Mishina M (1992). Identification by mutagenesis of a Mg^{2+}-block site of the NMDA receptor channel. *Nature* **358**, 673–675.

Nabekura J, Kawamoto I & Akaike N (1994). Developmental change in voltage dependency of NMDA receptor-mediated response in nucleus tractus solitarii neurons. *Brain Res* **648**, 152–156.

Nowak L, Bregestovski P, Ascher P, Herbet A & Prochiantz A (1984). Magnesium gates glutamate-activated channels in mouse central neurons. *Nature* **307**, 462–465.

Parsons CG, Danysz W, Bartmann A, Spielmanns P, Frankiewicz T, Hesselink M, Eilbacher B & Quack G (1999*a*). Amino-alkyl-cyclohexanes are novel uncompetitive NMDA receptor antagonists with strong voltage-dependency and fast blocking kinetics: in vitro and in vivo characterization. *Neuropharmacology* **38**, 85–108.

Parsons CG, Danysz W & Quack G (1999*b*). Memantine is a clinically well tolerated *N*-methyl-D-aspartate (NMDA) receptor antagonist – a review of preclinical data. *Neuropharmacology* **38**, 735–767.

Parsons CG, Gruner R, Rozenthal J, Millar J & Lodge D (1993). Patch-clamp studies on the kinetics and selectivity of *N*-methyl-D-aspartate receptor antagonism by memantine (1-amino-3,5-dimethyladamantan). *Neuropharmacology* **32**, 1337–1335.

Qian A, Antonov SM & Johnson JW (2002). Modulation by permeant ions of Mg^{2+} inhibition of NMDA-activated whole-cell currents in rat cortical neurons. *J Physiol* **538**, 65–77.

Qian A, Buller AL & Johnson JW (2005). NR2 subunit-dependence of NMDA receptor channel block by external Mg^{2+}. *J Physiol* **562**, 319–331.

Qian A & Johnson J (2006). Permeant ion effects on external Mg^{2+} block of NR1/2D NMDA receptors. *J Neurosci* **26**, 10899–10910.

Sakurada K, Masu M & Nakanishi S (1993). Alteration of Ca^{2+} permeability and sensitivity to Mg^{2+} and channel blockers by a single amino acid substitution in the *N*-methyl-D-aspartate receptor. *J Biol Chem* **268**, 410–415.

Vicini S, Wang JF, Li JH, Zhu WJ, Wang YH, Luo JH, Wolfe BB & Grayson DR (1998). Functional and pharmacological differences between recombinant N-methyl-D-aspartate receptors. *J Neurophysiol* **79**, 555–566.

Wollmuth LP, Kuner T & Sakmann B (1998). Adjacent asparagines in the NR2-subunit of the NMDA receptor channel control the voltage-dependent block by extracellular Mg $^{2+}$. *J Physiol* **506**, 13–32.

Woodhull AM (1973). Ionic blockage of sodium channels in nerve. *J Gen Physiol* **61**, 687–708.

Wyllie DJA, Béhé P & Colquhoun D (1998). Single-channel activations and concentration jumps: comparison of recombinant NR1a/NR2A and NR1a/NR2D NMDA receptors. *J Physiol* **510**, 1–18.

Wyllie DJA, Béhé P, Nassar M, Schoepfer R & Colquhoun D (1996). Single-channel currents from recombinant NMDA NR1a/NR2D receptors expressed in *Xenopus* oocytes. *Proc R Soc Lond B Biol Sci* **263**, 1079–1086.

Wyllie DJA & Chen PE (2007). Taking the time to study competitive antagonism. *Br J Pharmacol* **150**, 541–551.

Wyllie DJA, Johnston AR, Lipscombe D & Chen PE (2006). Single-channel analysis of a point mutation of a conserved serine residue in the S2 ligand binding domain of the NR2A NMDA receptor. *J Physiol* **574**, 477–489.

Zhu Y & Auerbach A (2001*a*). Na^{+} occupancy and Mg^{2+} block of the *N*-methyl-D-aspartate receptor channel. *J Gen Physiol* **117**, 275–286.

Zhu Y & Auerbach A (2001*b*). K^{+} occupancy of the *N*-methyl-D-aspartate receptor channel probed by Mg^{2+} block. *J Gen Physiol* **117**, 287–298.

Acknowledgements

This work was supported by a grant from the Biotechnology and Biological Sciences Research Council (15/C16800; D.J.A.W.) and funds from the Undergraduate Pharmacology Honours Programme at the University of Edinburgh.

Supplemental material

Online supplemental material for this paper can be accessed at:
http://jp.physoc.org/cgi/content/full/jphysiol.2007.143164/DC1
and
http://www.blackwell-synergy.com/doi/suppl/10.1113/jphysiol.2007.143164